Three-dimensional water diffusion and modelling of flax/shape memory epoxy composites

Li, Qinyu; Le Duigou, Antoine; Kumar Thakur, Vijay; Liu, Liwu; Leng, Jinsong; Scarpa, Fabrizio

Published in:
Composites Part A: Applied Science and Manufacturing

DOI:
10.1016/j.compositesa.2023.107574

First published: 01/08/2023

Document Version
Publisher's PDF, also known as Version of record

Composites: Part A 171 (2023) 107574

Contents lists available at ScienceDirect

Composites Part A

journal homepage: www.elsevier.com/locate/compositesa

Three-dimensional water diffusion and modelling of flax/shape memory epoxy composites

Qinyu Li [a], Antoine Le Duigou [b], Vijay Kumar Thakur [c], Liwu Liu [d], Jinsong Leng [e,*], Fabrizio Scarpa [a,*]

[a] Bristol Composites Institute, University of Bristol, BS8 1TR Bristol, UK
[b] Polymer and Composites, Bionic-group, Université Bretagne Sud, UMR CNRS 6027, IRDL, F-56100 Lorient, France
[c] Biorefining and Advanced Materials Research Centre, Scotland's Rural College (SRUC), Kings Buildings, West Mains Road, Edinburgh EH9 3JG, UK
[d] Department of Astronautical Science and Mechanics, Harbin Institute of Technology (HIT), P.O. Box 301, No. 92 West Dazhi Street, Harbin 150001, PR China
[e] National Key Laboratory of Science and Technology On Advanced Composites in Special Environments, Harbin Institute of Technology (HIT), No.2 Yikuang Street, P.O. Box 3011, Harbin 150080, PR China

ARTICLE INFO

Keywords:
Hygromorph composites
3D moisture diffusion
Flax fibre reinforced composites
Internal stresses

ABSTRACT

Current applications of mass diffusion in composite structures with natural fibres reinforcements focus on the development of large thickness, balanced laminates, and long diffusion times. Hygromorph composites are, however, thin in thickness and possess slender shapes with unbalanced laminate designs, together with higher moisture diffusion speeds. This work proposes a new three-dimensional inverse identification diffusion method based on extracting the diffusion parameters from each direction in hygromorph composites made of the shape memory epoxy and aligned long flax fibres. The proposed methodology is particularly suitable for slender hygromorphs composites, because the in-plane moisture diffusion is non-negligible in those cases. The method proposed here also helps the understanding of the moisture diffusion and associated mechanical deformations in general hygromorph adaptive morphing structures made of natural fibre-reinforced unbalanced composites.

1. Introduction

Natural fibre composites have been extensively studied and evaluated during the last decades because of their sustainability, low cost, low density, and interesting mechanical properties [1–4]. Moisture absorption tends to degrade the performance of the fibres in a composite [5]. This has motivated the development of several studies related to the water diffusion behaviour and its effects on the mechanical properties of natural fibre-reinforced composites, like those including flax [6,7,8,9,10], jute [11,12] and even hybrid flax/glass [13], flax/bamboo [14] and Kevlar/Cocos nucifera [15]. Most of the studies involving natural fibre composites are focused on semi-structural materials with relatively large thickness (3 mm or more), balanced laminates, long water diffusion times (3 weeks or more), and overall low levels of water uptake (less than 10 %) [6,7,10,11,12,13,14,15].

Natural fibre and moisture-responsive biocomposites are also promising as platforms for smart morphing materials [16–18]. The morphing mechanism is based on the different levels of hygroscopic expansion within the biologically inspired unbalanced laminates when the humidity changes. The internal stresses created from the moisture-induced swelling of the natural fibres through the thickness of the unbalanced laminate at different humidity conditions contribute to the bending actuation [19,20]. Natural fibre hygromorph composites used for actuation and sensing tend however to be slender and limited in thickness (around 0.5 mm) [16–18]. The architectures of these hygromorphs mainly consist of laminates with short diffusion times (around 3 h) and high overall water uptake (more than 10 %) [16–18]. The differences in terms of adsorption, mechanical and hygroscopic performance stem from the architectures and the composition of those composites: their volumetric fraction of fibres and stacking sequences, type of matrix and specimens' size, especially the thickness. Composites for morphing applications are designed with smaller thickness to absorb more moisture at higher speed. In contrast, composites with load-bearing applications (even secondary) aim to maintaining a structural integrity with improved protection from degrading moisture absorption. Unbalanced slender and medium thickness biocomposites, however, require further analysis of their water diffusion behaviour, also to improve the actuation authority performance and the evaluation of their

* Corresponding authors.
E-mail addresses: lengjs@hit.edu.cn (J. Leng), F.Scarpa@bristol.ac.uk (F. Scarpa).

https://doi.org/10.1016/j.compositesa.2023.107574
Received 21 February 2023; Received in revised form 3 April 2023; Accepted 11 April 2023
Available online 14 April 2023

residual and internal stresses.

Existing moisture diffusion studies applied to unbalanced biocomposites for actuation are limited [16–18]. All those referenced works are related to the application of the one-dimensional formulation of Fick's law, which is adopted because the dimensions of the samples along the thickness are significantly lower than the in-plane ones. Besides the sample scale effect, the lumen of unidirectional single flax fibres triggers imbibition, while moisture transport is promoted by capillarity along the longitudinal direction of the long fibres [21]. Those effects, however, are not described by a simple one-dimensional formulation of Fick's law. A three-dimensional Fick's law would however potentially describe in a more exhaustive manner the mass diffusion behaviour of hygromorph composites. The most common approach to obtain the diffusivity parameters along each composite direction is by using unsealed samples that absorb moisture from the three directions simultaneously, and by mathematically fitting the experimental curves to calculate the diffusivity parameters with minimum residuals [22–24]. However, the results of the diffusivity from the three different directions may have wide scatters, even when the relative errors are minimised. The minimum relative errors are obtained by changing D_1, D_2, D_3 (i.e., the diffusivity parameters from three directions) and M_∞ (the saturated moisture content) [7,23,25], or changing D_1, D_2, D_3 but keeping M_∞ is fixed [22,26]. The coupling between the diffusion from the different directions makes difficult to obtain an accurate inverse identification. Another approach followed in open literature is to measure the diffusivity separately along each direction and exposure condition [7,25,26]. The water diffusion in biobased composites is however complex, and the diffusion parameters identified from the sealed samples do not allow a direct description of the 3D water diffusion behaviour. The existing works show results in an agreement between each other when related to the final absorbed moisture content. Still, they are not conclusive about the time history of the 3D moisture absorption in hygromorph composites.

In the present work, we perform one-dimensional water diffusion experiments along the Cartesian directions of flax/epoxy hygromorph laminates to obtain diffusion coefficients for the three directions (the flax fibre longitudinal, transverse in-plane and through-the-thickness - see section 3.1). The diffusivity parameters obtained with this approach are related to the whole laminate, and therefore incorporate additional effects, like those provided by the porosity within the composites [27]. The relationship between the measured diffusivity is extended to the unsealed 3D cases, although the measured diffusivity parameters themselves cannot be directly applied to 3D cases, as other papers in open literature mention [22–24]. A 3D finite element model describing both balanced and unbalanced laminates is built and shows some significant agreement between the experimental and the numerical results when using the 3D diffusion model with the parameters identified with the described approach (section 3.2). The effects of the ply design and geometry are discussed (section 3.3) and the advantages of the new 3D diffusion identification model are described (section 3.4). The moisture distribution of those laminates is described using the benchmarked method and allows for a parametric analysis involving sizes and aspect

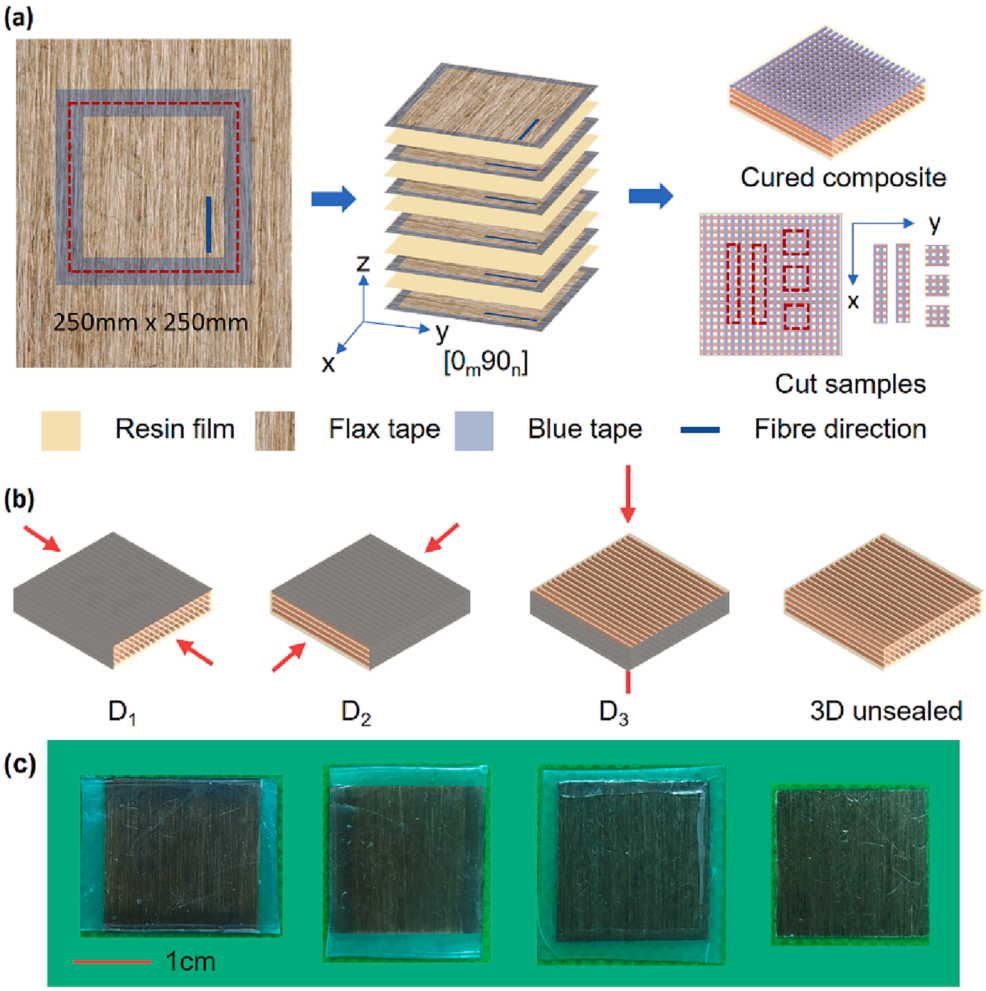

Fig 1. (a) Preparation and manufacturing layout of the flax/SMP epoxy composites. (b) Sealed and unsealed samples and principal directions of the water diffusion (1: fibre direction, 2: fibre transverse direction, and 3: thickness direction). (c) Sealed and unsealed specimens used for the measurements.

ratios of the composites (section 3.5). Based on the calculated moisture distributions, the internal stress distributions through the thickness direction of the unbalanced composites are also evaluated (section 3.6).

2. Materials and method

2.1. Materials and manufacturing process

Unidirectional flax fibre tapes (50 g/m^2) have been supplied by Natup (Flaxtape FT50). According to the manufacturer, no physical or chemical treatment has been carried out on the fibres harvested in France, then dew-retted, scutched, and hackled. Pure flax fibre tapes are fixed by blue tape (No.: 458–7141, RS Components, UK) on their boundaries and cut into 250 mm*250 mm size seeing Fig. 1. Stacks of shape memory epoxy films provided by Leng's Group [28] and unidirectional flax-fibre tapes (50 g/m^2) have been cured in autoclave with 0.69 MPa pressure and heated for 80 °C and 3 h, 100 °C (3 h) and 150 °C for 5 h. The blue tape used can sustain temperatures more than 150 °C. Eight-layer flax tapes are made in balanced [90_8] and unbalanced [$0_1 90_7$], [$0_2 90_6$] and [$0_3 90_5$] configurations. The [$0_m 90_n$] terms indicate m layers of laminas with fibres direction parallel to the X axis, and n layers with fibres parallel to Y axis. A Guillotine Cutter Trimmer Machine cuts the composite plates because of the thin thickness into small squares of 20 mm by 20 mm in size and stripes of 70 mm in length and 10 mm in width. The cured composites have ~ 0.56 mm thickness and 40 % fibre volume content and 15.6 ± 1.5 % porosity. The thickness is measured using a Mitutoyo micrometre IP65. The fibre volume content is measured by inspecting images of the composites cross-sections acquired using an optical ZEISS microscope, and the porosity is determined via gravimetric measurements in water. The water gravimetric method is easy and inexpensive; however, it overestimates the effective value of the porosity [27]. The samples cut from the [90_8] laminate are sealed to assess the effects of the anisotropy of the flax fibres composites. The samples (20 mm × 20 mm) cut from the laminate plates (250 mm × 250 mm) have been polished and sealed with Ethylene-vinyl acetate (EVA) to privilege the intended diffusion directions (1, 2 or 3 directions, with 1 being the fibre direction, 2 the transverse one and 3 the thickness direction). Fig. 1 (b) and (c) show images of the sealed and unsealed samples. The EVA material has been used for sealing because of it is water-resistant performance; no visible weight gain due to the presence of water was observable within 24 h.

2.2. Diffusion experiments

Manufactured and cut samples were stored prior to testing in a Votsch climatic chamber with controlled RH at 50 % and temperature at 23 °C. These conditions constitute the reference state, at which no environmental loading occurs. All specimens have been totally immersed in water at room temperature. The samples have then been removed from the water at regular intervals of immersion time. Those are 0.5, 1, 2, 3, 4, 6, 8, 10, 12, 14, 18, 24, 30, and 36 h. The samples have been wiped dry to remove the surface moisture, and then weighed using a balance with 10^{-3} g precision (PNS 600–3 Kern, Germany). An estimation of the total testing time and the suitable time interval to sample the weight of the specimen can be provided by carrying out preliminary trials. It is important to note that the specimens were weighed in a short time to minimize discontinuity effects during the water diffusion process. After an immersion time t, the amount of absorbed water W_t in the composite specimens was calculated to obtain the moisture content (MC) using the following expression:

$$MC(\%) = \frac{W_t - W_0}{W_0} \cdot 100 \tag{1}$$

In (1), W_t and W_0 are the weights of immersion in water over time and the dry material before immersion (for RH = 50 % and T = 23 °C).

The moisture content (MC) calculated for the sealed specimens covered by the EVA material has however a slightly different formulation:

$$MC(\%) = \frac{W_t - W_S}{W_0} \cdot 100 \tag{2}$$

In (2), W_t, W_S and W_0 are respectively the weights of immersion in water over time, the weight dry material with the sealed covering before immersion and the weight of the unsealed specimens without coverings.

It is worth noting that the results shown in section 5 represent the average values of at least five samples and a ± max/min standard deviation is also indicated.

3. Results and discussion

3.1. One directional water diffusion

The aim of this part is to measure the diffusion parameters of flax fibre composites from the experimental absorption curves and time history of the moisture content shown in Fig. 2. For each principal direction, only one diffusion coefficient can be identified using Fick's model (i.e., D_1, D_2, D_3). An analytical solution for the diffusivity is given by Crank [20] for thin plates, which provides a constant diffusion coefficient Eq. (3).

$$M_t = \left(1 - \frac{8}{\pi^2} \Sigma_{n=0}^{\infty} \frac{1}{(2n+1)^2} \exp\left(-D\left(\frac{2n+1}{e}\right)^2 \pi^2 t\right)\right) \times M_\infty \tag{3}$$

In (3), M_t indicates the time varying moisture content and t is the time. M_∞ represents the saturation moisture content (%) and D corresponds to the diffusion coefficient (mm^2/s). The term e represents the geometry parameter of the specimen through the diffusion direction.

The diffusion coefficients D along each principal direction of the unidirectional biobased composites are calculated by fitting this equation to the experimental data and minimizing the quadratic error q, sum of the difference between experimental and predicted values.

The saturation moisture content M_∞ slightly varies within the four cases (1, 2, 3 and unsealed cases). The initial diffusion speed affects the final sorption, so that unsealed samples absorb more moisture than the sealed ones. Sealed ones with higher initial diffusion speed conditions also absorb more than those with low-speed ones (direction 3 > direction 1 > direction 2). Two options from methodologies available in open literature can be selected to identify M_∞ when fitting the correspond D coefficients. The first consists in applying the experimental saturated moisture contents from each case [25]. The second involves the

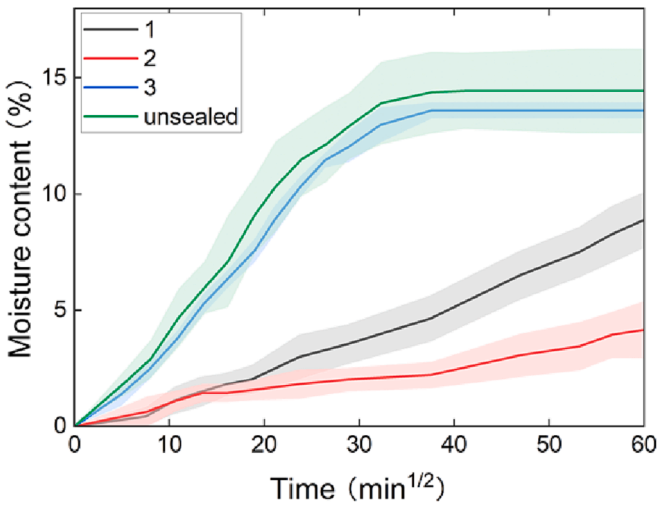

Fig 2. Evolution of the water uptake for the sealed (along the 1, 2 and 3 directions) and unsealed samples.

simultaneous identification of M_∞ and D to minimize the quadratic error q [7]. In the latter cases, the coefficients about the diffusion directions 1 and 2, M_∞ and D are fitted together because the inverse identification of M_∞ alone is computationally expensive, and there is lack of accurate experimental results related to M_∞. The diffusion experiments last 60 h but are still far away from reaching a complete absorption; on the contrary, the normal diffusion times to reach the complete diffusion in unsealed samples are just around 20 h. The sealed material (EVA) and the interfaces between the composites and the EVA films make the measured moisture growth larger than the one occurring. For the cases related to the diffusion direction 3 and the unsealed ones, the values of M_∞ are taken directly from the experiments. The terms D_1, D_2 and D_3 are calculated based on the values of M_∞ for each case. The results of the diffusion parameters from each direction and the saturated moisture uptake are shown in Table 1.

The diffusion coefficient along the 1 direction is much larger than the diffusion in the 2 and 3 directions, because direction 1 is related to the axis of the fibres. The term D_1 is found 133 times larger than D_3, and around 4 times greater than D_2, which is like existing results available for other epoxy and flax fibre composites [26]. The diffusion parameter along the thickness direction D_3 is selected as the baseline and the relationships between the other direction parameters and the baseline are indicated as R_1 and R_2; the latter coefficients show how many times the diffusion parameters D_1 and D_2 are larger (or smaller) than D_3. The difference between diffusion parameters is related to the fibre direction. Most plant fibres present a multi-scale porous structure with a main intrinsic porosity (lumen), which is filled with nutrients and emptied after the demise of the plant [29,30]. Smaller internal cavities of a few micrometres in diameter are also present [31]. Luminal porosity in flax fibres range from 1.6 % to 6.8 ± 3.5 % [29,32], highlighting some variations existing within the same type of flax plant fibres. Longitudinal direction allows the flax lumen to trigger imbibition and thus promotes water transport by capillarity [22]. Rapid water diffusion also occurs along natural fibres/matrix interfaces, which may be even faster than in the matrix itself [33,34]. Indeed, fibre/matrix interfaces generate complex interactions with moisture because their surface components (cellulose, hemicellulose, and pectin) promote water diffusion along the longitudinal direction of the fibre [33]. In addition, the matrix/fibre interface is also a preferential area for porosity to be formed (i.e., lack of wettability), which can further promote moisture transport and accumulation.

The method to seal the samples used in this work can only guarantee the initial specific diffusion direction, but not the control of that direction all the time. Matrices and fibres in load bearing biocomposites have different moisture transfer velocities and saturation contents: fibres transfer faster and absorb more moisture [23]. Hence, the moisture will also transfer from the fibres to their surrounding matrix and the measured parameters D_1, D_2 and D_3 cannot be directly extracted from 3D diffusion models.

3.2. D water diffusion

The full 3D solution to the Fickian diffusion behaviour with anisotropic diffusion coefficients is [35]:

$$M_t = \left(1 - \left(\frac{8}{\pi^2}\right)^3 \Sigma_{i=0}^{\infty}\Sigma_{j=0}^{\infty}\Sigma_{k=0}^{\infty} \frac{\exp\left(-\pi^2 t\left(D_1\left(\frac{2i+1}{a}\right)^2 + D_2\left(\frac{2j+1}{b}\right)^2 + D_3\left(\frac{2k+1}{c}\right)^2\right)\right)}{(2i+1)^2(2j+1)^2(2k+1)^2}\right) \times M_\infty \quad (4)$$

In (4) M_t is the moisture content that varies with the time t. M_∞ is the saturation moisture content (%) and D_i corresponds to the diffusion coefficient through the i direction (mm^2/s). a, b, c are the dimensions of the specimens through the 1, 2 and 3 diffusion directions.

The aim here of fitting the data to the full 3D model was to determine the values of the diffusivities D_1, D_2, D_3 and M_∞ of the unsealed specimens when immersed in the water, by minimizing the residuals. To carry out the identification of the diffusivities, 4 different methods have been applied:

I. Changing D_1, D_2, D_3 and M_∞ simultaneously to reach the minimum error [7,23,25];
II. Changing D_1, D_2, D_3, but keep the measured M_∞ to reach the minimum error [22,26];
III. Changing D_3, but maintain constant the measured M_∞ and scaled factors R_1, R_2 to reach the minimum error. This is the original method presented in this work;
IV. Use all parameters from the sealed experiments D_1, D_2, D_3 and M_∞ [25,26].

The fitting process is shown in the Fig. 3. The results of the identifications of the diffusivity parameters from these four methods are shown in Fig. 4(a) and Table 2. Method I) shows the best agreement between experiments, providing the minimum residual ($3.55*10^{-4}$) among all of them because of the most controlled parameters (D_1, D_2, D_3 and M_∞). Method II) also provides a low residual ($4.81*10^{-4}$) to control the fitting of D_1, D_2, D_3. However, the physical relevance of the parameters extracted from methods (I) and (II) are questionable. The fitted diffusion parameters are quite different from those obtained from the experiments on the sealed samples: for example, the value of D_1 value from the sealed experiment is 11.6 $*10^{-5}$ mm^2/s, while the analogous value extracted from the method I) is 118.2 $*10^{-5}$ mm^2/s. Also, values fitted following the same method have vast differences seeing Fig. 4(b): the diffusion parameters from I(1) and I(2) are completely different, but provide the exactly same overall moisture level. The same situation occurs between II(1) and II(2). The solution of methods (I and II) is not unique, because the moisture uptake evolution over time is dictated by the effect of coupling between the three directions (D_1, D_2, D_3) which has difficulty originating the separate contributions; The results are counterintuitive: D_3 should never be 0 and the coefficient D_1 should never be over 100 $*10^{-5}$ mm^2/s [7,22,23,25,26]. In summary: identifying the terms D_1, D_2, D_3 from fitting by using methods I and II is useful when coupling is present between the effects. It is not useful anymore when the contributions between the terms are separated.

The results from IV exhibit the largest errors. Some of the moisture diffusion works described in the open literature [25,26] confirm that the water diffusion in biobased composites is complex and the diffusion parameters identified from sealed samples do not allow a direct description of the 3D water diffusion behaviour. From the results of this work, method IV is recommended because the fitting of the terms D_1, D_2, D_3 are controlled by the ratios R_1 and R_2 that relate to the physical values from sealed experiments and minimize the overall error.

Table 1
Experimental values of diffusivity parametres D_i for the sealed samples along the three directions (1, 2 and 3).

D_1 (mm^2/s)	D_2(mm^2/s)	D_3(mm^2/s)	$R_1 = \frac{D_1}{D_3}$	$R_2 = \frac{D_2}{D_3}$
(1.16 ± 0.22) $*10^{-4}$	(3.09 ± 0.65) $*10^{-5}$	(8.69 ± 0.87) $*10^{-7}$	133.49	35.56

3.3. Effects of the ply design and geometry

Two types of samples with square (20 mm*20 mm) and long rectangle shapes (70 mm*10 mm) have been cut. Each type of specimen has

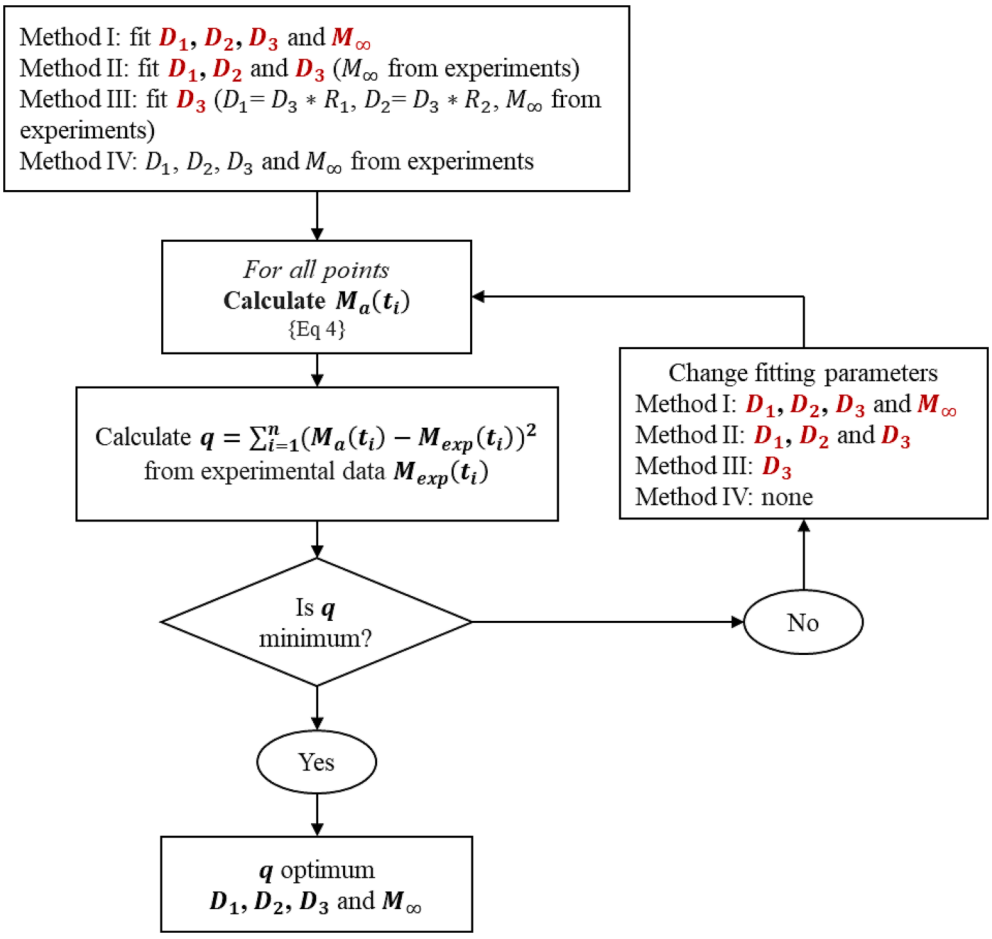

Fig 3. Schematic flow diagram describing how the directional diffusion coefficients have been determined for the four methods.

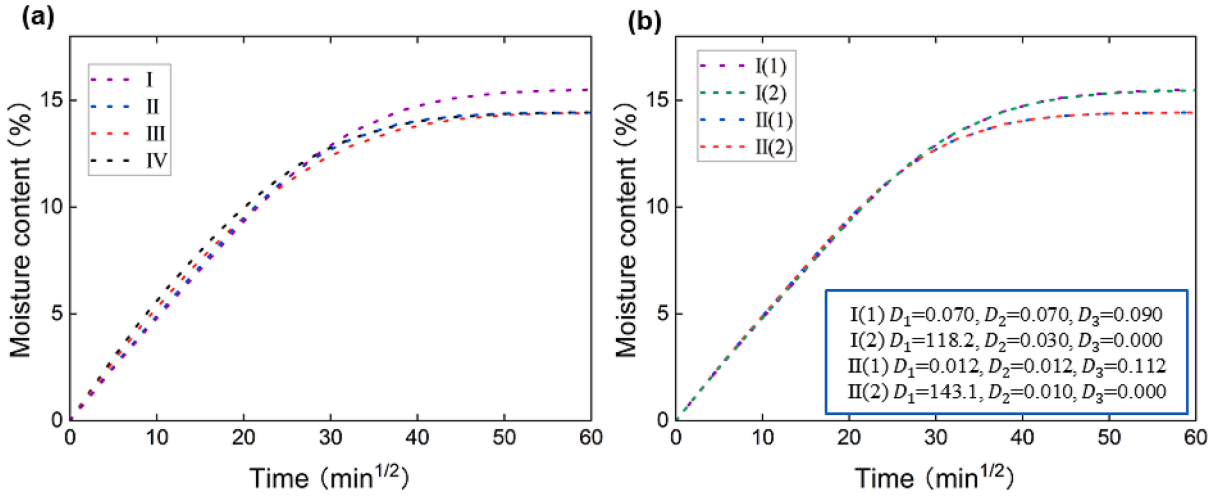

Fig. 4. (a) Results of the identification of the diffusivity parameters using the four methods of this paper. (b) Two set results of diffusion parameters D_1, D_2, D_3 from method I) or II) are significantly different. Those parameters however provide the same coupling effects during the identification process.

4 different laminates ($[90_8]$, $[0_190_7]$, $[0_290_6]$ and $[0_390_5]$). Sample L $[0_190_7]$ is indicative of long rectangle shapes samples with 70 mm (x) *10 mm (y) size. That sample also has 1 layer whose fibre direction is parallel to × axis and 7 layers parallel to y axis.

Different from balanced $[90_8]$ laminates, the x-axis and y-axis of the unbalanced specimens have both layers with fibres in the longitudinal and transverse direction. The global diffusion parameters D_x and D_y of the unbalanced samples mix the local diffusion parameters D_1 and D_2. The global diffusion parameters D_x and D_y are calculated by using a finite element approach in Abaqus 2018. The analysis type here is 'Mass diffusion'. The size of the model is 10 mm*10 mm*0.56 mm, a quarter of the experimental samples because the diffusion behaviours are considered symmetric. The model has been partitioned into two parts because of the unbalanced design and the local diffusion parameters D_1, D_2 and

Table 2
Fitting results related to the 4 methods. The shaded parts are the fitting parameters.

Method	D_1 (mm^2/s)*10^{-5}	D_2(mm^2/s)*10^{-5}	D_3(mm^2/s)*10^{-5}	M_∞(%)	Error (10^{-4})
I(1)	0.070	0.070	0.090	15.53	3.9007
I(2)	118.2	0.030	0.000	15.49	3.5514
II(1)	0.012	0.012	0.112	14.44	4.8120
II(2)	143.1	0.010	0.000	14.44	4.8145
III	D_3*R_1	D_3*R_2	0.077	14.44	9.8537
IV	11.58	3.09	0.087	14.44	11.8266

D_3 are derived from the method III. The FE models are made of 6400 elements (20*20 *16 from ×, y, z), with element type DC3D8. The loading method is like the one present in the 1D experiments, i.e., by sealing the boundary and collecting the overall moisture content from the specific direction (x, y and z) respectively, to fit the D_x, D_y and D_z values [23,24]. The loading at the boundary corresponds to the moisture concentration at saturation. The output of the model is the moisture concentration (CONC) of every element and the normalized concentration (NNC) of every node. The final fitting results of D_x, D_y and D_z and the relative relationships R_x and R_y are shown in Table 3. The D_{mix} (i.e., the global diffusion parameters D of the unbalanced samples from the mixing of D_1 and D_2) are larger if the percentage of D_1 is higher. Similar as other mixture theories, D_{mix} can be predicted as in equation (5). The predicted values of D_{mix} show a substantial agreement with the finite element results - see Fig. 5.

$$D_{mix} = D_1{}^*C_1 + D_2(1 - C_1) \tag{5}$$

In (5), D_{mix} is the global diffusion parameter of the unbalanced samples, while D_1 and D_2 are the local diffusion parameters along and transverse to the direction of the fibres; C_1 is the percentage of fibre direction layers.

After calculating the terms D_x and D_y related to the layers oriented at 0° and 90°, the new scaling factors R_x and R_y can be calculated. The new sets of diffusion parameters for different laminates and shapes are computed following method III in Table 4. The experimental results and the simulations are shown in the Fig. 6; square shapes and long rectangle samples are displayed in Fig. 6(a) and (b), respectively.

The experimental results show that the overall water uptake of the various cases is different, especially for different laminates (Table 3). The unbalanced laminates absorb more than the balanced ones. Composites with different fibre directions have a better moisture transfer along the various directions, and architectures with stacking sequences including fibres along multiple directions absorb more moisture than unidirectional ones [7]. In the case of unbalanced samples, the bending during the shape change also induces internal compressive stresses, which may help to increase the amount of moisture diffused [36]. The $[0_3 90_5]$ saturated moisture content is higher than $[0_2 90_6]$ and larger than the $[0_1 90_7]$ case, as also happens for the D_z terms. A scatter chart shows the relationship between M_∞ and D_z and the linear fitting is applied (Fig. 7 (a)). The scatters related to the S and L specimens cluster around a line. The predicted D_z (transparent points in the line) matches well the experimental results and the different errors within the fitting (orange colour) from method c. The predicted values of D_z from the linear fitting are compared in Fig. 7 (b). The small error increase related to the identified D_z values indicates that the saturated moisture content M_∞ is useful to predict the set diffusion parameters D_x, D_y and D_z within the same sample shape and different laminates.

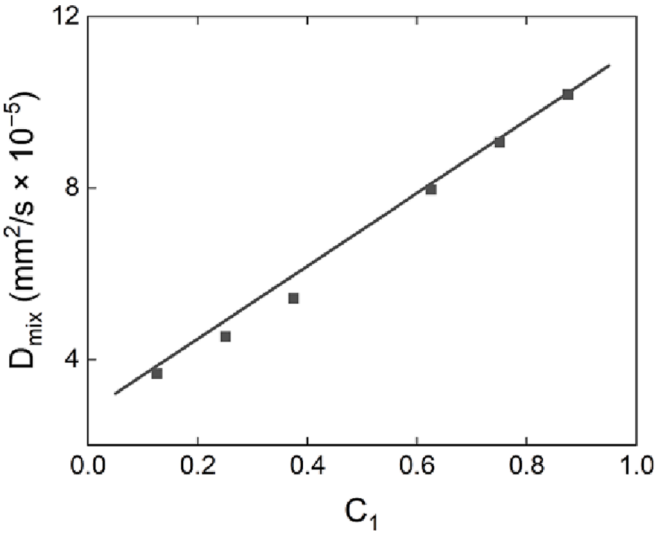

Fig. 5. Relationship between the global diffusion parameters D_{mix} of the unbalanced hygromorphs and the percentage of layers C_1 containing fibres oriented at 0°. The dotted points are derived from the finite element simulation, while the continuous line represents eq. (5).

3.4. Advantages of the 3D diffusion model

The thickness of hygromorph composites used to achieve high curvature ranges is usually very small compared to their planar sizes. Most of the current hygromorphs designed for actuation are based on diffusion along the thickness, because the small thickness dimensions are mostly instrumental to the moisture transfer [16–18]. However, besides the effects due to the geometry of the hygromorphs, the diffusion parameters along the fibres longitudinal direction also play an important role that should not be overlooked. To highlight this point, Fig. 8 shows a Venn Diagram about the evolution of the moisture content being transferred along the planar and through-the-thickness directions for S $[90_8]$ laminates with different sizes. The data in the Venn diagram are based on the diffusion parameters shown in Table 4. The values of the moisture gains in the plane of the hygromorph (i.e, the overall area without the thickness absorption) and the overall moisture absorption (total area) are also marked. During transient, a non-negligible amount of moisture comes from the length and width directions, and this indicates the usefulness of adopting a 3D diffusion model for hygromorph composites. In the case of square hygromorphs (20 mm*20 mm), the moisture along the y direction is larger than along the × one, because the

Table 3
The global diffusion parameters D_x, D_y are affected by the ply design and the new relative relationship through different directions R_x and..R_y

Samples	D_1 (mm^2/s)*10^{-5}	D_2(mm^2/s)*10^{-5}	D_3(mm^2/s)*10^{-5}	D_x (mm^2/s)*10^{-5}	D_y(mm^2/s)*10^{-5}	D_z(mm^2/s)*10^{-5}	R_x	R_y
$[90_8]$	D_3*R_1	D_3*R_2	D_3	D_2	D_1	D_3	R_2	R_1
$[0_1 90_7]$				1.32*D_2	0.90*D_1		47.08	120.54
$[0_2 90_6]$				1.63*D_2	0.80*D_1		58.03	107.33
$[0_3 90_5]$				1.95*D_2	0.70*D_1		69.45	94.24

Table 4
Global diffusion parameters D_x, D_y and D_z for different laminates and the error between the fitting results and practical experiments.

Laminates	D_x (mm^2/s)*10^{-5}	D_y(mm^2/s)*10^{-5}	D_z(mm^2/s)*10^{-5}	M_∞(%)	Error (10^{-4})
S[90_8]	D_z*R_x	D_z*R_y	0.077	14.44	9.8537
S[$0_1 90_7$]			0.093	18.03	2.3544
S[$0_2 90_6$]			0.128	21.47	23.2464
S[$0_3 90_5$]			0.140	22.14	18.4924
L[90_8]			0.095	14.18	3.7325
L[$0_1 90_7$]			0.149	17.24	1.9681
L[$0_2 90_6$]			0.152	19.42	3.4011
L[$0_3 90_5$]			0.202	21.80	1.9388

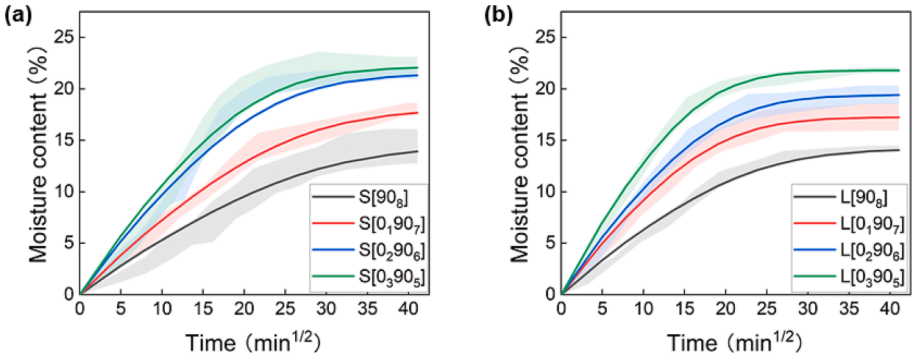

Fig 6. Experimental evolution of the water uptake for the square (S) and long rectangle (L) shaped hygromorphs with different stacking sequences and the predicting results (lines) by the 3D diffusion model. (a) square cases and (b) long rectangle cases.

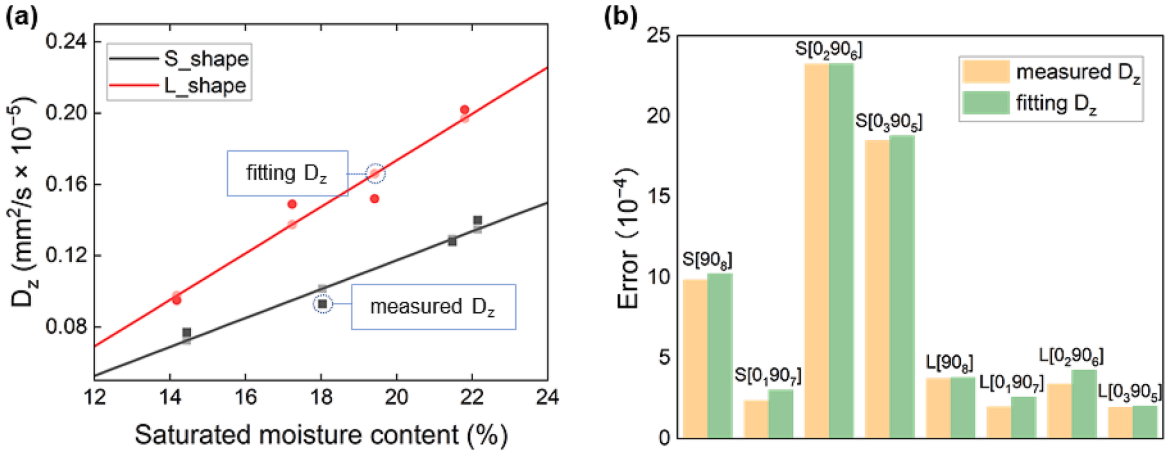

Fig 7. Relationship between saturated moisture content M_∞ and the diffusion parameter D_z. Comparison of errors between experimentally measured D_z (orange) and linear fitting D_z (green). (For interpretation of the references to colour in this figure legend, the reader is referred to the web version of this article.)

y axis is parallel to the longitudinal direction of the fibres. For samples with rectangular shape, the shorter the × and y directions, the more significant role the in-plane effect plays. Existing published works on composite natural fibre hygromorphs describe actuators that have widths exactly of 10 mm [16–18], which indicate that non-negligible in-plane diffusion effects do exist. If narrower samples are designed with 5 mm of width, the moisture from the fibre direction is larger than in the case of the thickness one (Fig. 8. 70 mm*5mm case). It is important to notice that the in-plane diffusivity effects are stronger during the transient phase of the actuation. During the first 0.25 h, the in-plane diffusivity for the 70 mm X 5 mm hygromorph accounts for ~ 52 % of the total diffusion within the biobased composite, and this ratio decreases to ~ 37 % when the width of the hygromorph is double (10 mm). After 4 h, the planar diffusivity accounts for ~ 40 % for the slenderest hygromorph, and to 26 % for the 10 mm width one. Only a steady state (16 h), the final contribution of the planar diffusivity is minor (~9% for the hygromorph with 10 mm width).

The hygromorphs examined in this example all have a small thickness (0.56 mm), compared to their in-plane dimensions. Nonetheless, 3D-based moisture diffusion behaviours appear more descriptive of the different phases of the moisture-induced actuation than equivalent 1D models applied to the thickness direction only.

3.5. Moisture distribution with the 3D model

3.5.1. Square versus long rectangle shapes

The moisture distribution along the 3 directions within balanced [90_8] laminates of square (20 × 20 mm) and long rectangle shapes (70 × 10 mm) is computed using the Finite Element model (Fig. 9). The simulations are carried out using the modified diffusivity parameters shown in Table 4. Here the longitudinal direction of the fibres is along the y axis. The selected time intervals are 0.25, 1, 4 and 16 h. The

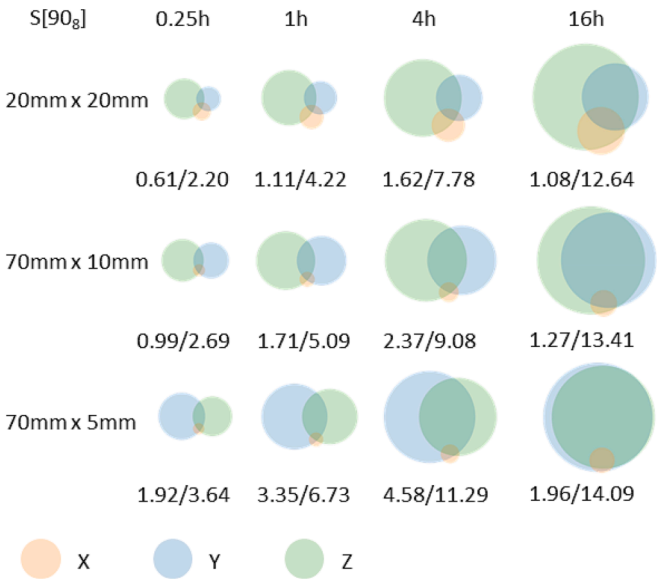

Fig 8. Venn plots of the moisture distribution through the ×, y and z directions for square and rectangle-shaped hygromorph samples with a [90$_8$] stacking sequence. For each diffusion time, the values a/b indicate a as the overall moisture absorption minus from the thickness direction (overall area minus Z area); b is the overall moisture absorption (total area).

moisture concentration in the model is extracted at each node and averaged within the cross-sections normal to the ×, y and z directions. The moisture distribution results are not equal through the × or y directions, reflecting the presence of edge effects within the Finite Element model. The position near the in-plane edge absorbs higher moisture than in the middle part and the higher amount of moisture would not be identified if the simple 1D diffusivity model is applied. For the S[90$_8$] samples, the moisture absorption along the z direction is larger than in the y and the × ones. The reason behind this behaviour is the very thin size along the z direction (0.56 mm) and the highest diffusivity (Table 4) in the y direction. In the L[90$_8$] cases, the y direction plays a more important role because of the shorter size (from 20 mm to 10 mm), while the × direction effects are less important (increase of the length to 70 mm). For example, during a 4 h diffusion time, the moisture through the y direction in the S[90$_8$] laminate is small in the middle part. This however does not occur for the L[90$_8$] laminate, which has a nearly flat shape like the S[90$_8$] but possesses an evident curved behaviour.

3.5.2. *Balanced versus unbalanced architectures*

Unbalanced laminates are not common architectures of natural fibre composites [6,7,8,9,10,11,12,13,14,15], however the laminate with the [0$_3$90$_5$] stacking sequence is treated here as example. Like balanced laminates, the water distribution through the thickness increases from the middle to the top or bottom laminas. The laminas of an unbalanced laminate are numbered from 1 to 7 (Fig. 10**)**. The parts shown in the figure represent one-quarter of the composite, because the rest of the structure is symmetric. The diffusion time here is 1 h. The results shown are related to the normalized concentration of moisture at each node (NNC) of the Finite Element model. The unbalanced stacking sequence also makes the water diffusion unbalanced. The fibres in laminas #1 and #2 absorb more along the longitudinal direction (i.e., the fibre directions), while laminas #6 and #7 absorb more along the transverse direction (which also correspond to the uniaxial direction of the fibres); this behaviour is also more evident in laminas #2 and #6. Lamina #3 is special, because it connects the reinforcing flax fibres from two directions; that is why the amount of absorbed water is larger than the one in lamina #5 in the longitudinal direction, but it is similar in the transverse one.

3.5.3. *Different hygromorph stacking sequences*

The distribution of the moisture content in slender rectangular flax/epoxy hygromorphs with different stacking sequences ([0$_1$90$_7$], [0$_2$90$_6$] and [0$_3$90$_5$]) is shown in Fig. 11. The experimental results show that their amounts of water uptake are different (Fig. 8) and that also the diffusivity along the three main directions differ. The distribution of the moisture content through the thickness is also slightly unbalanced. The overall moisture in the laminas with fibres interfacing at the two

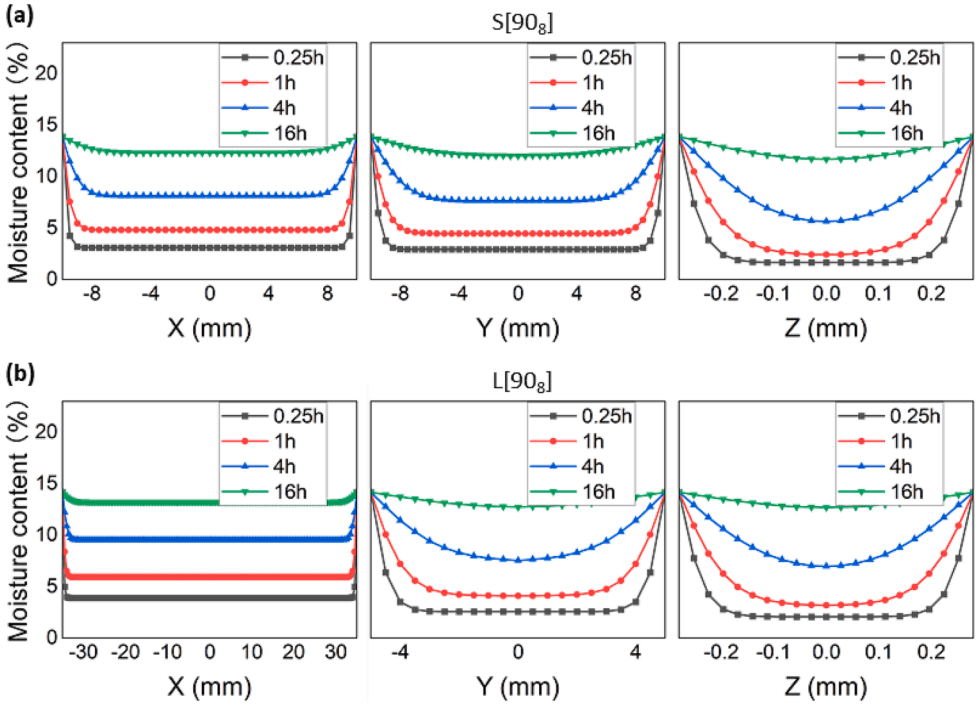

Fig 9. Moisture distribution through ×, y and z directions of square (S) and long (L – 70 mm X 10 mm) rectangle shaped samples with the [90$_8$] stacking sequence.

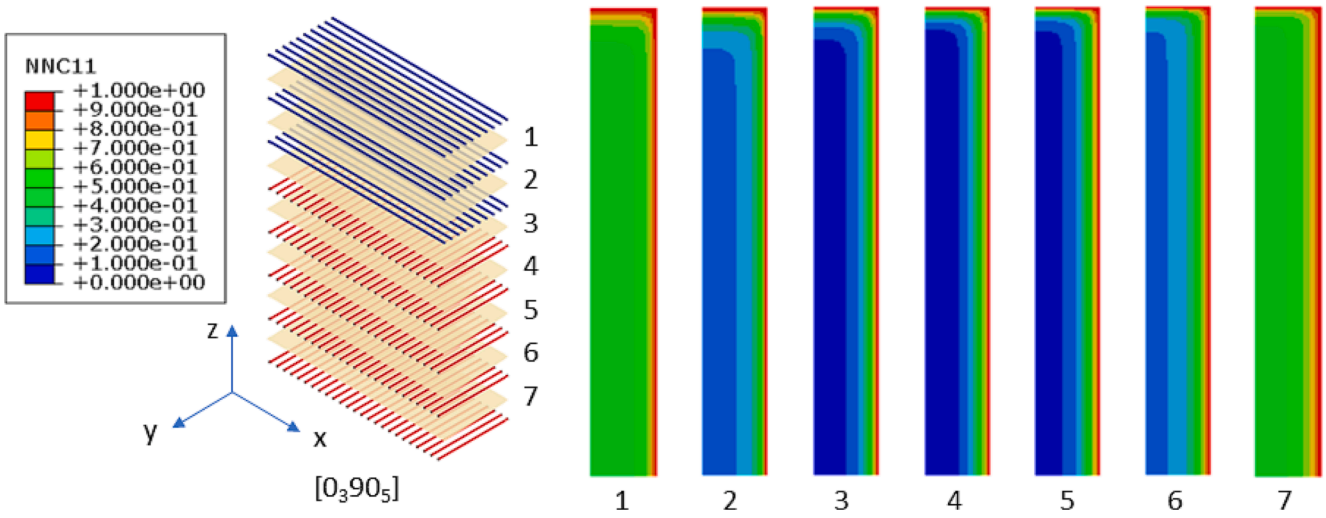

Fig 10. The composite architecture of $[0_3 90_5]$ laminates and the colourmap of the normalized concentration of the through-the-thickness moisture distribution.

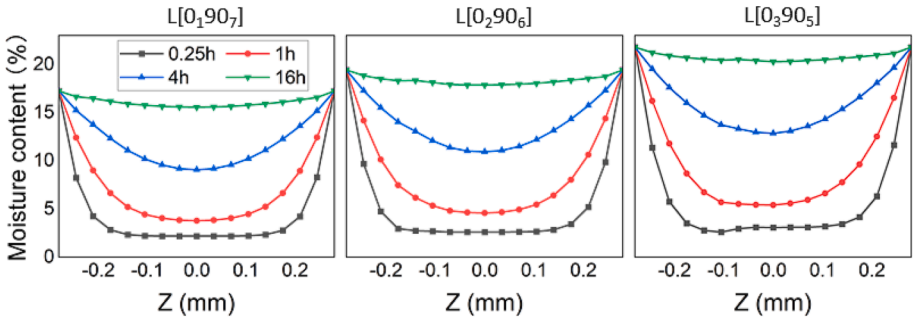

Fig 11. Through-the-thickness moisture distribution in unbalanced $[0_1 90_7]$, $[0_2 90_6]$ and $[0_3 90_5]$ hygromorph composites.

orthogonal directions is always larger than in the case of the symmetric laminates (Fig. 9).

3.6. Hygromorph performance of the flax/SMP epoxy composites

3.6.1. Hygroscopic expansion

Hygroscopic expansion and moisture uptake have been evaluated on samples 70 mm (L) × 10 mm (w) × 0.56 mm (t). The size of those samples is the same as the one of the specimens used to observe the moisture sensitive morphing. Volumetric measurements have been performed with a Mitutoyo micrometre IP65 and gravimetric analyses using a Fischer Scientific PAS214C balance (10^{-3} g). The coefficient of hygroscopic expansion (β) was determined as the slope of the hygroscopic expansion over the MC. The results are shown in Fig. 12 (a) [16].

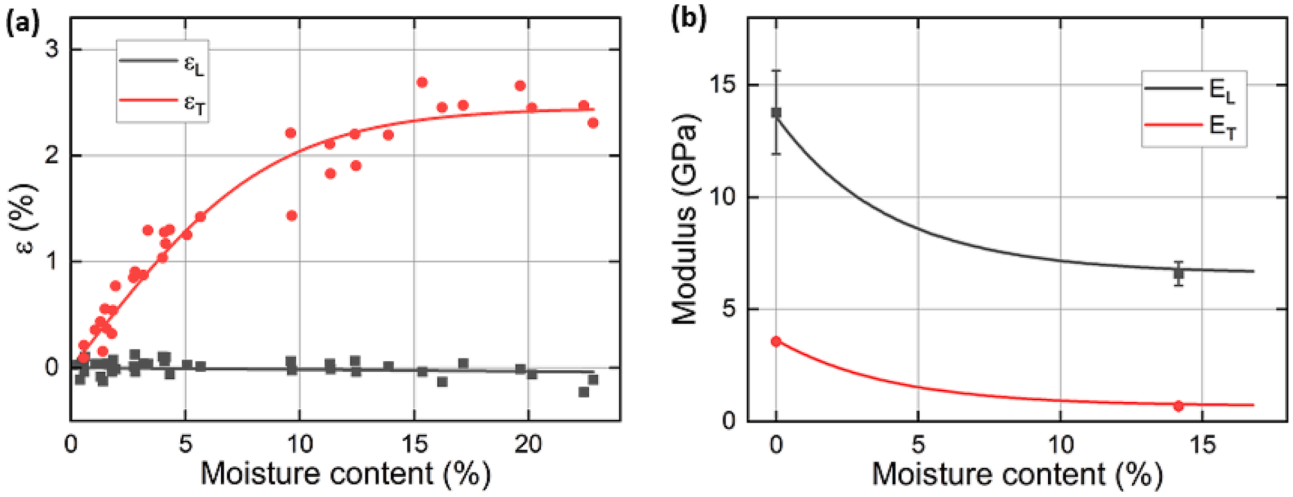

Fig 12. (a) Evolution of the longitudinal and transverse hygroscopic strains at 20 °C. Black (longitudinal) and red (transverse) dots represent the experimental data. The continuous lines refer to the theoretical results from the model. (b) Evolution of the longitudinal and transverse Young's moduli as a function of moisture content. (For interpretation of the references to colour in this figure legend, the reader is referred to the web version of this article.)

Along the fibre direction, the hygroscopic expansion is insensitive to the moisture and even shows a very slight shrinkage. In contrast, the biocomposites along the fibre transverse direction have a large expansion, because the fibres in the radial direction swell when absorbing moisture. The coefficient of hygroscopic expansion decreases with the moisture absorption and the overall expansion reaches 2.39 % from 50 % RH to a well absorbed condition.

3.6.2. Hygroelastic properties

The tensile properties of dry and wet unidirectional biocomposites with flax fibre orientation set at 0° (E_L) and 90° (E_T) were measured separately according to ISO 527–4 standards, by using a Shimadzu universal testing machine (cell load 5 kN) at controlled temperature (23 °C) and crosshead speed of 1 mm/min. The samples have the following dimensions (thickness θ and width w): $\theta_{0°}$=0.56 mm and width $w_{0°}$=15 mm; $\theta_{90°}$=0.56 mm and $w_{90°}$= 25 mm. Mechanical tests were performed on samples that had reached their saturation time, estimated at 24 h. The samples were wrapped with polymer film to prevent the loss of moisture. An axial extensometer with a nominal length of 25 mm (L_0) was used to measure the strain. The tensile modulus was determined within a range of strains between 0.05 and 0.1 % [16]. The tensile moduli in fibre direction decreases from 13.8 GPa at 50 % RH to 6.6 GPa fully immersed in the water. In the transverse direction, the analogous values varied from 3.5 GPa at 50 % RH to 0.7 GPa. The loss of mechanical performance is significant before absorbing 10 % of moisture content but slows down after that moisture content value. The experimental data related to the mechanical properties illustrated here are at 50 % RH and immersed state, and the trend shown are like other hygromorphs described in open literature [19,20].

3.6.3. Curvatures

To measure the radius of curvature, markers were tracked on images captured using a camera (1080P HD, 30fps) and image analysis was performed using Autodesk software. At specific instants of time, images are extracted from the video clips and the related curvatures are measured. The curvature was measured by fitting the time history of the sample profile to a circle function. The bending curvature (K) was calculated with the radius of the fitted circle. The video illustrating the morphing of the hygromorph is recorded (Supplementary video) and the clips are shown in Fig. 13(a). The time history of the fitted curvatures from the video tracking and the calculated results predicted by using a modified version of the Timoshenko equation [18,20] are shown in Fig. 13(b).

3.6.4. Stress distribution

The distributed moisture contributes to the level of internal stresses in biocomposites. The hygroscopic expansion relationship between moisture content and expansion ratio are found in [16]. The same geometry and the same mesh are used for obtaining a static solution. The moisture concentration at each node is the input loading, and the material properties contain the expansion ratio and the values of the tensile moduli versus the moisture content. The distribution of the internal hygroscopic stresses through the laminate thickness is shown in Fig. 14. The largest stress (tensile or compressive) happens close to the interface between the 0° and 90° plies, no matter the laminate architecture considered. The σ_{xx} stress close to the interface of those laminas first increase, and then decreases over time. The reason for this is due to the decrease of the tensile modulus of flax composite materials with the moisture uptake [16,18,20], although the hygroscopic strain increases continuously. In the different types of laminates, the values of σ_{xx} stress in the steady state (green line) at the interface decrease with the decrease of the number of 90° plies because 90° laminas create hygroscopic differential strains, and 0° laminas bear those generated hygroscopic strains.

4. Conclusion

In this work, flax fibres reinforced epoxy hygromorph composites have been manufactured and subjected to diffusion experiments to identify the parameters D_1, D_2, D_3 and M_∞. Scaling factors $R_1 = D_1/D_3$ and $R_2 = D_2/D_3$ have been used within the formulation of 3D diffusion models. Agreement between experimental and analytical models is observed for both the balanced and unbalanced architectures of the biocomposites when investigating two types of samples shapes (20 mm *20 mm and 70 mm *10 mm) and four different laminates design ($[90_8]$, $[0_190_7]$, $[0_290_6]$ and $[0_390_5]$). The effects of the diffusion with the different laminates designs and the geometry of composites are evaluated, with particular emphasis on the time history of the moisture distribution through the thickness and the internal stresses distribution by hygroscopic expansion.

The proposed new method to obtain diffusivity parameters is discussed in comparison with the existing 3D diffusion methods. The method proposed in this work is particularly suitable for slender hygromorphs, because the planar moisture diffusion in those biobased composites is nonnegligible. The diffusion model proposed in this work also helps to understand the moisture diffusion behaviours and mechanisms in general hygromorph composites and adaptive morphing structures derived from those natural fibre-reinforced composites.

CRediT authorship contribution statement

Qinyu Li: Conceptualization, Methodology, Formal analysis,

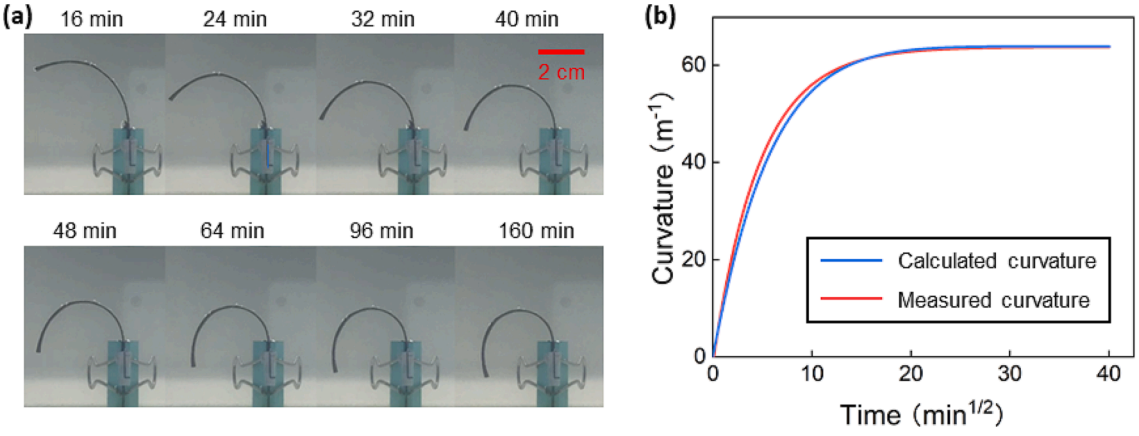

Fig 13. (a) Snapshots of hygromorphism over time (b) Evolution of the curvatures for the samples immersed in water. The calculated and measured curvatures show a good agreement.

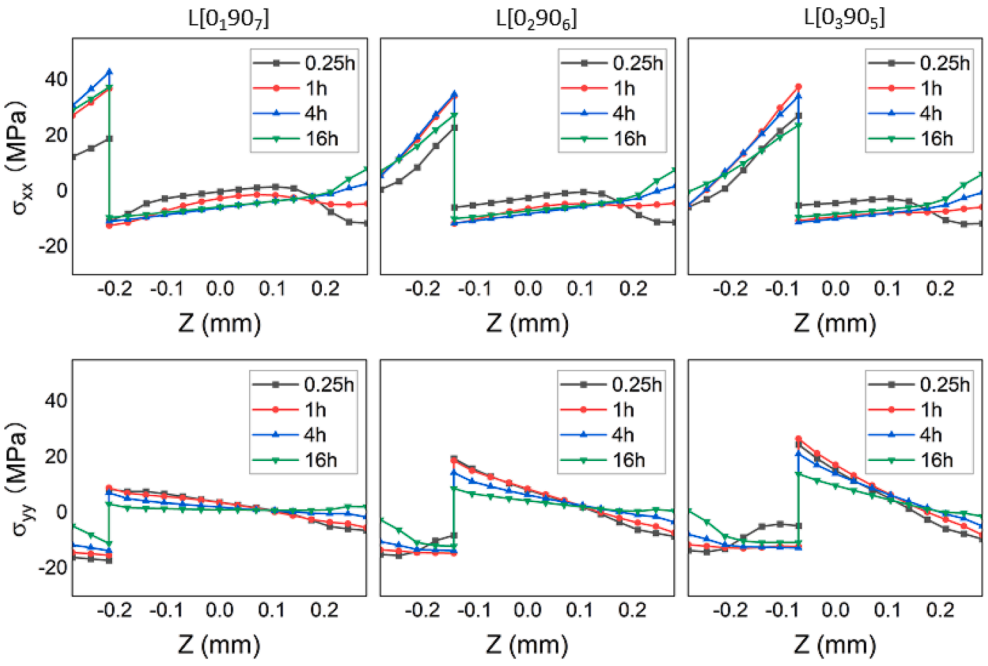

Fig 14. Stress distributions through the thickness for the unbalanced $[0_1 90_7]$, $[0_2 90_6]$ and $[0_3 90_5]$ hygromorphs.

Investigation, Visualization, Data curation, Writing – original draft. **Antoine Le Duigou:** Formal analysis, Investigation, Supervision, Writing – original draft. **Vijay Kumar Thakur:** Formal analysis, Writing – original draft. **Liwu Liu:** Investigation. **Jinsong Leng:** Resources, Investigation. **Fabrizio Scarpa:** Conceptualization, Formal analysis, Supervision, Resources, Project administration, Funding acquisition.

Declaration of Competing Interest

The authors declare that they have no known competing financial interests or personal relationships that could have appeared to influence the work reported in this paper.

Data availability

Data will be made available on request.

Acknowledgements

QL is grateful for the support of the Faculty of Engineering of the University of Bristol. FS acknowledges the logistical support of the H2020 BBI SSUCHY project for the use of the flax fibres and the composites manufacturing facilities. FS also acknowledges the support of the ERC-2020-AdG 101020715 NEUROMETA project.

Appendix A. Supplementary material

Supplementary data to this article can be found online at https://doi.org/10.1016/j.compositesa.2023.107574.

References

[1] Rajak DK, Pagar DD, Menezes PL, Linul E. Fiber-reinforced polymer composites: manufacturing, properties, and applications. Polym 2019;11. https://doi.org/10.3390/polym11101667.
[2] Shah DU, Porter D, Vollrath F. Can silk become an effective reinforcing fibre? A property comparison with flax and glass reinforced composites. Compos Sci Technol 2014;101:173–83.
[3] Mohanty AK, Vivekanandhan S, Pin JM, Misra M. Composites from renewable and sustainable resources: challenges and innovations. Science 2018;362:536–42.
[4] Ramesh M, Palanikumar K, Reddy KH. Plant fibre based bio-composites: sustainable and renewable green materials. Renew Sustain Energy Rev 2017;79:558–84.
[5] Lau K, Hung P, Zhu M-H, Hui D. Properties of natural fibre composites for structural engineering applications. Compos Part B Eng 2018;136:222–33.
[6] Muñoz E, García-Manrique JA. Water absorption behaviour and its effect on the mechanical properties of flax fibre reinforced bioepoxy composites. Int J Polym Sci 2015;2015:390275.
[7] Saidane EH, Scida D, Assarar M, Ayad R. Assessment of 3D moisture diffusion parameters on flax/epoxy composites. Compos Part A Appl Sci Manuf 2016;80:53–60.
[8] dos Santos JC, de Oliveira LA, Panzera TH, Remillat CDL, Farrow I, Placet V, et al. Ageing of autoclaved epoxy/flax composites: Effects on water absorption, porosity and flexural behaviour. Compos Part B Eng 2020;202:108380.
[9] Fiore V, Calabrese L, Miranda R, Badagliacco D, Sanfilippo C, Palamara D, et al. On the response of flax fiber reinforced composites under salt-fog/dry conditions: Reversible and irreversible performances degradation. Compos Part B Eng 2022;230:109535.
[10] Prasad V, Sekar K, Joseph MA. Mechanical and water absorption properties of nano TiO_2 coated flax fibre epoxy composites. Constr Build Mater 2021;284:122803.
[11] Akil HM, Cheng LW, Mohd Ishak ZA, Abu Bakar A, Abd Rahman MA. Water absorption study on pultruded jute fibre reinforced unsaturated polyester composites. Compos Sci Technol 2009;69:1942–8.
[12] Doan T-T-L, Brodowsky H, Mäder E. Jute fibre/polypropylene composites II. Thermal, hydrothermal and dynamic mechanical behaviour. Compos Sci Technol 2007;67:2707–14.
[13] Saidane EH, Scida D, Assarar M, Sabhi H, Ayad R. Hybridisation effect on diffusion kinetic and tensile mechanical behaviour of epoxy based flax–glass composites. Compos Part A Appl Sci Manuf 2016;87:153–60.
[14] Alliyankal Vijayakumar A, Prasad V, Kailathuvalappil KM. Investigation on the effect of stacking order and hybridization on mechanical and water absorption properties of woven flax/bamboo composites. Polym Compos 2022;43:5189–207.
[15] Naveen J, Jawaid M, Zainudin ES, Sultan MTH, Yahaya R. Mechanical and moisture diffusion behaviour of hybrid Kevlar/Cocos nucifera sheath reinforced epoxy composites. J Mater Res Technol 2019;8:1308–18.
[16] Li Q, Sun R, Le Duigou A, Guo J, Rossiter J, Liu L, et al. Programmable and reconfigurable hygro-thermo morphing materials with multifunctional shape transformation. Appl Mater Today 2022;27:101414.
[17] Le Duigou A, Keryvin V, Beaugrand J, Pernes M, Scarpa F, Castro M. Humidity responsive actuation of bioinspired hygromorph biocomposites (HBC) for adaptive structures. Compos Part A Appl Sci Manuf 2019;116:36–45.
[18] Le Duigou A, Requile S, Beaugrand J, Scarpa F, Castro M. Natural fibres actuators for smart bio-inspired hygromorph biocomposites. Smart Mater Struct 2017;26:125009.
[19] Péron M, Célino A, Jacquemin F, Le Duigou A. Hygroscopic stresses in asymmetric biocomposite laminates submitted to various relative humidity conditions. Compos Part A Appl Sci Manuf 2020;134:105896.
[20] Péron M, Célino A, Castro M, Jacquemin F, Le Duigou A. Study of hygroscopic stresses in asymmetric biocomposite laminates. Compos Sci Technol 2019;169:7–15.

[21] Richely E, Bourmaud A, Placet V, Guessasma S, Beaugrand J. A critical review of the ultrastructure, mechanics and modelling of flax fibres and their defects. Prog Mater Sci 2022;124:100851.
[22] Arnold JC, Alston SM, Korkees F. An assessment of methods to determine the directional moisture diffusion coefficients of composite materials. Compos Part A Appl Sci Manuf 2013;55:120–8.
[23] Chilali A, Assarar M, Zouari W, Kebir H, Ayad R. Analysis of the hydro-mechanical behaviour of flax fibre-reinforced composites: Assessment of hygroscopic expansion and its impact on internal stress. Compos Struct 2018;206:177–84.
[24] Jiang X, Kolstein H, Bijlaard F, Qiang X. Effects of hygrothermal aging on glass-fibre reinforced polymer laminates and adhesive of FRP composite bridge: Moisture diffusion characteristics. Compos Part A Appl Sci Manuf 2014;57:49–58.
[25] Chilali A, Assarar M, Zouari W, Kebir H, Ayad R. Effect of geometric dimensions and fibre orientation on 3D moisture diffusion in flax fibre reinforced thermoplastic and thermosetting composites. Compos Part A Appl Sci Manuf 2017;95:75–86.
[26] Djellouli B, Zouari W, Assarar M, Ayad R. Analysis of the hygroscopic and hygroelastic behaviours of water aged flax-epoxy composite. Compos Struct 2021;265:113692.
[27] de Kergariou C, Le Duigou A, Popineau V, Gager V, Kervoelen A, Perriman A, et al. Measure of porosity in flax fibres reinforced polylactic acid biocomposites. Compos Part A Appl Sci Manuf 2021;141:106183.
[28] Leng J, Wu X, Liu Y. Effect of a linear monomer on the thermomechanical properties of epoxy shape-memory polymer. Smart Mater Struct 2009;18:95031.
[29] Charlet K, Jernot JP, Eve S, Gomina M, Bréard J. Multi-scale morphological characterisation of flax: From the stem to the fibrils. Carbohydr Polym 2010;82:54–61. https://doi.org/10.1016/j.carbpol.2010.04.022.
[30] Madsen B, Gamstedt EK. Wood versus plant fibers: similarities and differences in composite applications. Adv Mater Sci Eng 2013;2013.
[31] Hernandez-Estrada A, Reza M, Hughes M. The structure of dislocations in hemp (Cannabis sativa L.) fibres and implications for mechanical behaviour. BioResources 2020;15:2579–95.
[32] Aslan M, Chinga-Carrasco G, Sørensen BF, Madsen B. Strength variability of single flax fibres. J Mater Sci 2011;46:6344–54. https://doi.org/10.1007/s10853-011-5581-x.
[33] Le Duigou A, Davies P, Baley C. Exploring durability of interfaces in flax fibre/epoxy micro-composites. Compos Part A Appl Sci Manuf 2013;48:121–8. https://doi.org/10.1016/j.compositesa.2013.01.010.
[34] Réquilé S, Le Duigou A, Bourmaud A, Baley C. Interfacial properties of hemp fiber/epoxy system measured by microdroplet test: Effect of relative humidity. Compos Sci Technol 2019;181:107694. https://doi.org/10.1016/j.compscitech.2019.107694.
[35] Jost W. Diffusion in solids. Liq Gases 1960;73.
[36] Humeau C, Davies P, Jacquemin F. Moisture diffusion under hydrostatic pressure in composites. Mater Des 2016;96:90–8. https://doi.org/10.1016/j.matdes.2016.02.012.